On topological properties of massless fermions in a magnetic field

Lemut, G.

Note: To cite this publication please use the final published version (if applicable).

5 Chiral charge transfer along magnetic field lines in a Weyl superconductor

5.1 Introduction

Three-dimensional Weyl fermions have a definite chirality, given by the $\pm$ sign in the Weyl Hamiltonian $\pm \boldsymbol{p} \cdot \boldsymbol{\sigma}$. Three spatial dimensions are essential, if $\boldsymbol{p} \cdot \boldsymbol{\sigma} = p_x \sigma_x + p_y \sigma_y$ contains only two Pauli matrices, then $+\boldsymbol{p} \cdot \boldsymbol{\sigma}$ and $-\boldsymbol{p} \cdot \boldsymbol{\sigma}$ can be transformed into each other by a unitary transformation (conjugation with σ_z). The chirality is therefore a characteristic feature of 3D Weyl semimetals, not shared by 2D graphene.

The search for observable signatures of chirality is a common theme in the study of this new class of materials [13, 66, 90, 91]. The basic mechanism used for that purpose is the chirality dependent motion in a magnetic field: Weyl fermions in the zeroth Landau level propagate parallel or antiparallel to the field lines, dependent on their chirality [92]. A population imbalance between the two chiralities then produces the chiral magnetic effect [93, 94]: An electrical current along the field lines, which changes sign if the field is inverted.

Here we present a novel, albeit less dramatic, signature of chirality: An electrical conductance which depends on the magnetic field direction. The effect appears if superconductivity is induced in a magnetic topological insulator, in the layered geometry of Meng and Balents [6] (see Fig. 7.1). The superconductor cannot gap out the Weyl points of opposite chirality, provided that the induced pair potential Δ_0 remains smaller than the magnetization energy β. The main effect of the superconductor is to renormalize the charge of the quasiparticles [95], by a factor $\kappa = \sqrt{1 - \Delta_0^2 / \beta^2}$.

A magnetic field B perpendicular to the layers penetrates in an array of $h/2e$ vortices. The zeroth Landau level is a dispersionless flat band in the plane of the layers — the chirality of the Weyl fermions prevents broadening of the Landau band by vortex scattering [96].
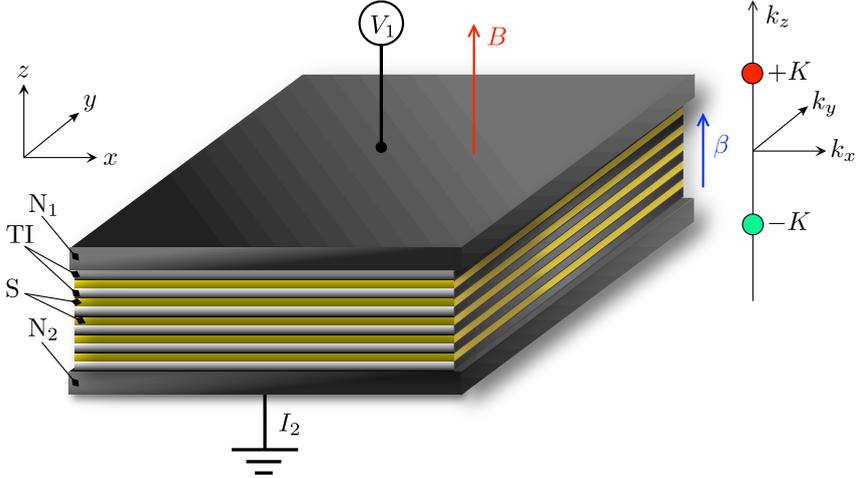
Figure 5.1: Left panel: Weyl superconductor formed by alternating layers of magnetic topological insulator (TI, magnetization β) and s-wave superconductor (S, pair potential Δ_0, chemical potential μ), between normal-metal contacts (N$_1$ and N$_2$. A magnetic field B perpendicular to the layers (along z) produces a Landau band that is dispersionless in the x–y plane, with free propagation in the z-direction. Right panel: Weyl points of opposite chirality at $k_z = \pm K$. For $\mu \neq 0$ the conductance $G = I_2/V_1$ depends on whether the magnetic field points parallel or antiparallel to the vector from $-K$ to $+K$.

Following Ref. 97 we probe the Landau band by electrical conduction: A voltage V_1 applied to contact N$_1$ induces a current $I_2 = GV_1$ in contact N$_2$. This is a three-terminal circuit, the grounded superconductor being the third terminal. The chemical potential μ_N in the normal-metal contacts is assumed to be large compared to the value μ in the superconductor. We calculate the dependence of the conductance $G(\pm B)$ on the direction of the magnetic field B, relative to the separation of the Weyl points of opposite chirality.

When the chemical potential is at the Weyl point ($\mu = 0$) the conductance is determined by the renormalized charge and B only enters via the Landau band degeneracy [97],

$$G = \kappa^2 G_0, \quad G_0 = (e^2/h)N_\Phi, \quad \text{at} \quad \mu = 0, \tag{5.1}$$

with $N_\Phi = eBS/h$ the flux through an area S in units of h/e. We generalize this result to nonzero μ and find that

$$\delta G = G(B) - G(-B) = (4\mu/\beta)(\kappa^2 - \kappa)G_0. \tag{5.2}$$

The conductance thus depends on whether the magnetic field points from $+$ chirality to $-$ chirality, or the other way around.

The outline of the chapter is as follows. In the next section we formulate the problem of electrical conduction along the magnetic vortices of a Weyl superconductor. The key quantity to calculate is the charge e^* transferred by the quasiparticles across the normal-superconductor interface. At $\mu = 0$ this is simply given by the renormalized charge κe of the Weyl fermions [97], but that no longer holds at nonzero μ. In Secs. 5.3 and 5.4 we apply a mode matching technique developed in Ref. 98 to calculate e^*. The conductance then follows in Sec. 5.5. These are all analytical results, we test them on a computer simulation of a tight-binding model in Sec. 6.A. We conclude in Sec. 7.6.

5.2 Weyl superconductor in a magnetic vortex lattice

We consider a three-dimensional Weyl superconductor [6] (Fermi velocity v_{F}, chemical potential μ, s-wave pair potential $\Delta_0 e^{i\phi}$), sandwiched between metal contacts N_1 and N_2 at $z = \pm L/2$ (see Fig. 7.1). A magnetic field $B > 0$ in the z-direction penetrates the superconductor in the form of a vortex lattice. The superconducting phase ϕ winds by 2π around each vortex (at position $\boldsymbol{R}_n$),

$$\nabla \times \nabla \phi = 2\pi \hat{z} \sum_n \delta(\boldsymbol{r} - \boldsymbol{R}_n). \tag{5.3}$$

The Bogoliubov-De Gennes Hamiltonian is

$$\begin{aligned}
\mathcal{H} = {} & v_{\mathrm{F}} \nu_z \tau_z (\boldsymbol{k} \cdot \boldsymbol{\sigma}) - e v_{\mathrm{F}} \nu_0 \tau_z (\boldsymbol{A} \cdot \boldsymbol{\sigma}) + \nu_0 \tau_0 \boldsymbol{\beta} \cdot \boldsymbol{\sigma} \\
& - \mu \nu_z \tau_0 \sigma_0 + \Delta_0 (\nu_x \cos \phi - \nu_y \sin \phi) \tau_0 \sigma_0.
\end{aligned} \tag{5.4}$$

The Pauli matrices $\sigma_\alpha, \tau_\alpha, \nu_\alpha$ act respectively on the spin, subband, and electron-hole degree of freedom. We set $\hbar$ to unity and choose the electron charge as $+e$. The magnetization $\boldsymbol{\beta} = \beta \boldsymbol{n}_\beta$ (with $\boldsymbol{n}_\beta$ a unit vector) may point in an arbitary direction relative to $\boldsymbol{B} = \nabla \times \boldsymbol{A} = B\hat{z}$. We choose a gauge in which $A_z = 0$ and both $\boldsymbol{A}$ and ϕ are z-independent.

The Weyl points in zero magnetic field are at momentum $\boldsymbol{k} = \pm \boldsymbol{K} = \pm K \boldsymbol{n}_\beta$ with

$$v_{\mathrm{F}} K = \kappa \beta, \quad \kappa = \sqrt{1 - \Delta_0^2/\beta^2}. \tag{5.5}$$

The Weyl cones remain gapless provided that $\Delta_0 < \beta$. In a magnetic field the states condense into Landau bands, dispersionless in the plane perpendicular to $\boldsymbol{B}$, but freely moving along $\boldsymbol{B}$.

A quasiparticle in a Landau band, at energy E, has charge expectation value $Q = -e\partial E/\partial\mu$. At the Weyl point, $\mu = 0 = E$, this equals [95]

$$Q_0 = \kappa e = e\sqrt{1 - \Delta_0^2/\beta^2}. \tag{5.6}$$

We seek the charge e^* transferred into the normal-metal contact by a quasiparticle in the Landau band. At $\mu = 0$ this was calculated in Ref. 97, with the result $e^* = Q_0$. We wish to generalize this to nonzero μ. For that purpose we apply a methodology developed for a different problem in Ref. 98, as described in the next section.

5.3 Fractional charge transfer

5.3.1 Matching condition

The particle current operator $\hat{v}_z$ and charge current operator $\hat{j}_z$, both in the z-direction, are given by

$$\begin{aligned}
\hat{v}_z &= \partial\mathcal{H}/\partial k_z = v_{\mathrm{F}}\nu_z\tau_z\sigma_z, \\
\hat{j}_z &= -\partial\mathcal{H}/\partial A_z = ev_{\mathrm{F}}\nu_0\tau_z\sigma_z.
\end{aligned} \tag{5.7}$$

In what follows we set v_{F} and e equal to unity, for ease of notation.

The chirality $\chi = \pm 1$ of a mode in the superconductor (S) determines whether it propagates in the $+z$ direction or in the $-z$ direction. We position the normal-superconductor (NS) interface at $z = 0$, so that the mode in S approaches it from $z < 0$ for $\chi = +1$ and from $z > 0$ for $\chi = -1$.

We assume that the chemical potential μ_{N} in N is large compared to the value μ in S. The potential step at the NS interface boosts the momentum component k_z perpendicular to the interface, without affecting the parallel components k_x, k_y, so in N only modes are excited with $|k_z| \gg |k_x|, |k_y|$. These are eigenstates of $\nu_z\tau_z\sigma_z$ with eigenvalue χ, moving away from the interface in the $+z$ direction if $\chi = +1$ and in the $-z$ direction for $\chi = -1$. Continuity of the wave function Ψ at the interface then gives the matching condition

$$\nu_z\tau_z\sigma_z\Psi = \chi\Psi \ \text{ at } \ z = 0. \tag{5.8}$$

5.3.2 Projection

Because the Hamiltonian (7.5) commutes with τ_z we can replace this Pauli matrix by the subband index $\tau = \pm 1$ and rewrite the matching condition (5.8) as $\chi\tau\nu_z\sigma_z\Psi = \Psi$. We define the projection operator

$$\mathcal{P} = \tfrac{1}{2}(1 + \chi\tau\nu_z\sigma_z), \;\; \text{such that} \;\; \mathcal{P}\Psi = \Psi \;\; \text{at} \;\; z = 0, \qquad (5.9)$$

and project the Hamiltonian (7.5),

$$\mathcal{P}\mathcal{H}\mathcal{P} = (\tau\beta_z - \chi\mu)\mathcal{P}\hat{j}_z\mathcal{P} + \mathcal{P}\hat{k}_z\hat{v}_z\mathcal{P}. \qquad (5.10)$$

We have used that $\boldsymbol{A}$ only has components in the x–y plane. The hat on $\hat{k}_z = -i\partial/\partial z$ is there to remind us it is an operator.

We take the z-dependent inner product

$$\langle\Psi_1|\Psi_2\rangle_z = \int dx \int dy \, \Psi_2^*(x,y,z)\Psi_2(x,y,z) \qquad (5.11)$$

of Eq. (5.10),

$$(\tau\beta_z - \chi\mu)\langle\Psi|\mathcal{P}\hat{j}_z\mathcal{P}|\Psi\rangle_z = \langle\Psi|\mathcal{P}\delta\mathcal{H}\mathcal{P}|\Psi\rangle_z,$$
$$\text{with} \;\; \delta\mathcal{H} = \mathcal{H} - \hat{k}_z\hat{v}_z. \qquad (5.12)$$

At the NS interface $z = 0$ the projector may be removed,

$$(\tau\beta_z - \chi\mu)\langle\Psi|\hat{j}_z|\Psi\rangle_0 = \langle\Psi|\delta\mathcal{H}|\Psi\rangle_0, \qquad (5.13)$$

since neither $\hat{j}_z$ nor $\delta\mathcal{H}$ contain a z-derivative, so that these operators commute with the limit $z \to 0$ and we may replace $\mathcal{P}\Psi$ by Ψ in view of the matching condition (5.9). Eq. (5.13) is the key identity that allows us to calculate the transferred charge.

5.3.3 Transferred charge

Let Ψ be an eigenstate of $\mathcal{H}$ at energy E. The transferred charge e^* through the NS interface is given by the ratio

$$e^* = \frac{\langle\Psi|\hat{j}_z|\Psi\rangle_0}{\langle\Psi|\hat{v}_z|\Psi\rangle_0}. \qquad (5.14)$$

Substitution of Eq. (5.13) equates this to

$$e^* = (\tau\beta_z - \chi\mu)^{-1}\frac{\langle\Psi|\mathcal{H} - \hat{k}_z\hat{v}_z|\Psi\rangle_0}{\langle\Psi|\hat{v}_z|\Psi\rangle_0} \qquad (5.15a)$$

$$= (\tau\beta_z - \chi\mu)^{-1}\left(\chi E - \frac{\langle\Psi|\hat{k}_z\hat{v}_z|\Psi\rangle_0}{\langle\Psi|\hat{v}_z|\Psi\rangle_0}\right). \qquad (5.15b)$$

The term χE appears because

$$\langle\Psi|\mathcal{H}|\Psi\rangle_0 = E\langle\Psi|\Psi\rangle_0 = \chi E\langle\Psi|\hat{v}_z|\Psi\rangle_0, \tag{5.16}$$

where in the last equality we used the matching condition (5.8).

Particle current conservation requires that

$$\frac{d}{dz}\langle\Psi|\hat{v}_z|\Psi\rangle_z = 0. \tag{5.17}$$

More generally, for our case of a z-independent Hamiltonian it holds that

$$\frac{d}{dz}\langle\Psi|f(\hat{k}_z)\hat{v}_z|\Psi\rangle_z = 0 \tag{5.18}$$

for any function of f of $\hat{k}_z$ (see App. 5.A for a proof). Each of the two expectation values $\langle\cdots\rangle_0$ on the right-hand-side of Eq. (5.15b) can thus be replaced by $\langle\cdots\rangle_z$. This ratio can then be evaluated for large $|z|$, far from the NS interface, where evanescent waves have decayed and $\Psi \propto e^{ik_z z}$ is an eigenstate of $\hat{k}_z$.

We finally obtain the transferred charge

$$e^* = e\frac{\chi E - v_{\mathrm{F}}k_z}{\tau\beta_z - \chi\mu}, \tag{5.19}$$

reinstating units of e and v_{F}. For $\mu = 0 = E$, $\beta = \beta_z$, $k_z = K = \kappa\beta/v_{\mathrm{F}}$ we recover the result $e^* = \pm\kappa e = \pm Q_0$ of Ref. 97.

It remains to relate the momentum k_z of a propagating mode at the Fermi level to the parameters of the Weyl superconductor. For that we need the dispersion relation $E(k_z)$ of the Landau band, which we calculate in the next section.

5.4 Dispersion relation of the Landau band

5.4.1 Block diagonalization

We calculate the dispersion relation of the Landau band by means of the block diagonalization approach of Ref. 96. Starting from the BdG Hamiltonian (7.5) we first make the Anderson gauge transformation [99]

$$\mathcal{H} \mapsto \Omega^\dagger\mathcal{H}\Omega, \;\; \text{with} \;\; \Omega = \begin{pmatrix} e^{i\phi} & 0 \\ 0 & 1 \end{pmatrix}. \tag{5.20}$$

The subblocks of Ω refer to the electron-hole (ν_α) degree of freedom. The resulting Hamiltonian is

$$\mathcal{H} = \nu_z \tau_z (\boldsymbol{k} + \boldsymbol{a}) \cdot \boldsymbol{\sigma} + \nu_0 \tau_z \boldsymbol{q} \cdot \boldsymbol{\sigma} + \nu_0 \tau_0 \boldsymbol{\beta} \cdot \boldsymbol{\sigma}$$
$$- \mu \nu_z \tau_0 \sigma_0 + \Delta_0 \nu_x \tau_0 \sigma_0, \tag{5.21}$$
$$\boldsymbol{a} = \tfrac{1}{2} \nabla \phi, \quad \boldsymbol{q} = \tfrac{1}{2} \nabla \phi - \boldsymbol{A}. \tag{5.22}$$

Both fields $\boldsymbol{a}$ and $\boldsymbol{q}$ have only components in the x–y plane and are z-independent.

To focus on states near $\boldsymbol{K}$ we set $\boldsymbol{k} = \kappa \boldsymbol{\beta} + \delta \boldsymbol{k}$ and consider $\delta \boldsymbol{k}$ small. The component parallel to $\boldsymbol{\beta}$ of a vector $\boldsymbol{v}$ is denoted by $v_\parallel = \boldsymbol{v} \cdot \boldsymbol{n}_\beta$.

One more unitary transformation $\mathcal{H} \mapsto U^\dagger \mathcal{H} U$ with

$$U = \sigma_\parallel \exp\left(\tfrac{1}{2} i \alpha \nu_y \tau_z \sigma_\parallel\right),$$
$$\tan \alpha = -\frac{\Delta_0}{K}, \quad \cos \alpha = -(1 + \Delta_0^2/K^2)^{-1/2} = -\kappa, \tag{5.23}$$

followed by a projection onto the $\nu = \tau = \pm 1$ blocks, gives a pair of 2×2 low-energy Hamiltonians,

$$H_\tau = \tau \kappa \mu \sigma_0 - (\delta \boldsymbol{k} + \boldsymbol{a} - \tau \kappa \boldsymbol{q}) \cdot \boldsymbol{\sigma}$$
$$+ (1 - \kappa)(\delta k_\parallel + a_\parallel + \tau q_\parallel) \sigma_\parallel. \tag{5.24}$$

Eq. (5.24) is an anisotropic Dirac Hamiltonian, the velocity parallel to the magnetization is reduced by a factor κ. The same factor renormalizes the quasiparticle charge,

$$Q = -e \frac{\partial H_\tau}{\partial \mu} = -e \tau \kappa. \tag{5.25}$$

The two Hamiltonians $H_\tau = H_\pm$ near $\boldsymbol{k} = \boldsymbol{K}$ thus describe quasiparticles of opposite charge. Another pair of oppositely charged Weyl cones exists near $\boldsymbol{k} = -\boldsymbol{K}$.

If $\boldsymbol{\beta} = (\beta \sin \theta, 0, \beta \cos \theta)$ makes an angle θ with the magnetic field we have

$$H_\tau = \tau \kappa \mu \sigma_0 - \sum_{\alpha = x,y} (\delta k_\alpha + a_\alpha - \tau \kappa q_\alpha) \sigma_\alpha - \delta k_z \sigma_z$$
$$+ (1 - \kappa)(\delta k_x \sin \theta + \delta k_z \cos \theta + a_x \sin \theta + \tau q_x \sin \theta)(\sigma_x \sin \theta + \sigma_z \cos \theta), \tag{5.26}$$

where we used that $a_z = 0 = q_z$.

5.4.2 Zeroth Landau band

A major simplification appears if the magnetization $\boldsymbol{\beta}$ and the magnetic field $\boldsymbol{B}$ are either parallel or perpendicular, so $\cos\theta \equiv \gamma \in \{0, \pm 1\}$. In these cases the Hamiltonian (5.26) anticommutes with σ_z when $\mu = 0 = \delta k_z$. This socalled chiral symmetry implies that the zeroth Landau band is an eigenstate of σ_z, with eigenvalue $-\tau$ [96]. The dispersion relation then follows immediately,

$$
\begin{aligned}
E(k_z) &= \tau\kappa\mu + \tau\delta k_z[1 - (1 - \kappa)\gamma^2] \\
&= \chi\kappa\mu + \chi(k_z - \kappa\beta\gamma)[1 - (1 - \kappa)\gamma^2].
\end{aligned} \tag{5.27}
$$

In the second equation we have identified the chirality index $\chi \equiv \text{sign}\,(dE/dk_z) = \tau$.

Equating $E(k_z) = E$ and solving for k_z gives

$$
k_z = \kappa\beta\gamma - \frac{\kappa\mu - \chi E}{1 - (1 - \kappa)\gamma^2}, \tag{5.28}
$$

to first order in E and μ. (Higher order terms are not captured by the linearization around the Weyl point.)

We substitute Eq. (5.28) in the expression (5.19) for the transferred charge,

$$
e^* = \frac{\chi e}{\mu - \beta\gamma}\left(\kappa\beta\gamma - \frac{\kappa\mu - \chi E}{1 - (1 - \kappa)\gamma^2} - \chi E\right). \tag{5.29}
$$

For $\boldsymbol{\beta} \parallel \boldsymbol{B}$ this gives

$$
e^* = -\chi e\,\frac{\pm\kappa\beta - \mu + \chi E(1/\kappa - 1)}{\pm\beta - \mu}, \quad \gamma = \pm 1. \tag{5.30}
$$

In contrast, for $\boldsymbol{\beta} \perp \boldsymbol{B}$ the μ and E dependence drops out,

$$
e^* = -\chi\kappa e, \quad \gamma = 0. \tag{5.31}
$$

These are the results for the charge transferred by a mode with k_z near $+K$. The mode with k_z near $-K$ is its charge-conjugate, the transferred charge is given by $e^*(E) \mapsto -e^*(-E)$.

5.4.3 Comparison of transferred charge and charge expectation value

For the case $\chi = 1$ that $\boldsymbol{\beta}$ is parallel to $\boldsymbol{B}$ we can use the more accurate dispersion relation from Ref. 96, without making the linearization around
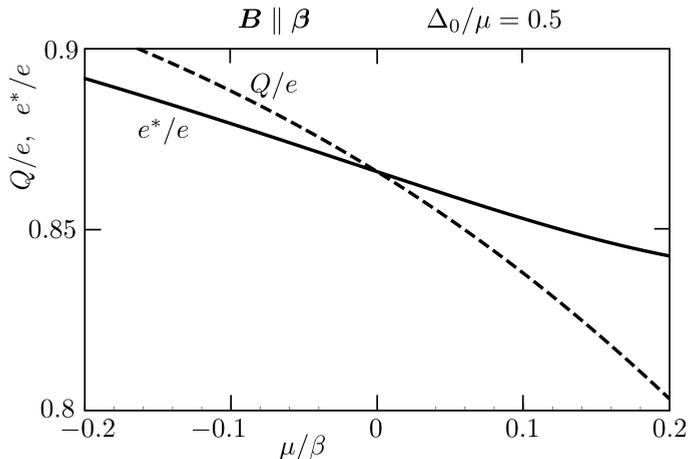
Figure 5.2: Comparison of the transferred charge e^* across the NS interface and the charge expectation value Q of the Weyl fermions. The curves are computed from Eqs. (5.33) and (5.36a) using k_0 from the full nonlinear dispersion (5.32).

the Weyl point:

$$E(k_z) = -\chi M(k_z) - \chi M'(k_z)\mu, \quad M(k_z) = \beta - \sqrt{\Delta_0^2 + k_z^2}. \qquad (5.32)$$

The solution $k_z = k_0(\mu)$ of the equation $E(k_z) = 0$ then gives the transferred charge at the Fermi level ($E = 0$) via

$$e^* = -\chi e \frac{k_0(\mu)}{\beta - \mu}. \qquad (5.33)$$

As a check for the linearization, to first order we find

$$k_0(\mu) = \sqrt{\beta^2 - \Delta_0^2} - \mu + \mathcal{O}(\mu^2), \qquad (5.34)$$

in agreement with Eq. (5.28) for $E = 0$, $\gamma = 1$. We checked that higher order terms are relatively insignificant for $|\mu/\beta| \lesssim 0.1$.

The resulting transferred charge

$$e^* = -\chi e \kappa \big[1 + (\mu/\beta)(1 - 1/\kappa) + \mathcal{O}(\mu^2)\big] \qquad (5.35)$$

can be compared with the charge expectation value

$$Q = \chi e M'(k_0) = -\frac{\chi e k_0}{\sqrt{\Delta_0^2 + k_0^2}} \qquad (5.36a)$$

$$= -\chi e \kappa \big[1 + (\mu/\beta)(\kappa - 1/\kappa) + \mathcal{O}(\mu^2)\big], \qquad (5.36b)$$

see Fig. 6.4. We conclude that the μ-dependence of the transferred charge e^* is not simply accounted for by the μ-dependence of the charge expectation value Q.

5.5 Conductance

5.5.1 Transmission matrix

The Landau band contains $N_\Phi = eBS/h$ modes propagating along the magnetic field through a cross-sectional area S. For each of these modes the transmission matrix $t(E)$ at energy E from contact N_1 to N_2 is a rank-two matrix of the form

$$t(E) = e^{ik_z L}|\Psi_2^+\rangle\langle\Psi_1^+| + e^{-ik_z L}|\Psi_2^-\rangle\langle\Psi_1^-|. \tag{5.37}$$

The incoming mode $|\Psi_1^\pm\rangle$ from contact N_1 is matched in S to a Landau band mode at $\pm k_z$. This chiral mode propagates over a distance L to contact N_2, picking up a phase $e^{\pm ik_z L}$, and is then matched to an outgoing mode $|\Psi_2^\pm\rangle$. The matching condition gives a charge $\pm e^*(\pm E)$ to $\Psi_n^\pm$,

$$\langle\Psi_n^\pm|\nu_z|\Psi_n^\pm\rangle = \pm e^*(\pm E). \tag{5.38}$$

The transmission matrix $t(E)$ has electron and hole submatrices t_{ee} and t_{he} (transmission of an electron as an electron or as a hole). These determine the differential conductance

$$\frac{dI_2}{dV_1} = G_0 \lim_{E \to eV_1} \text{Tr}\left(t_{ee}^\dagger t_{ee} - t_{he}^\dagger t_{he}\right)$$
$$= \tfrac{1}{2}G_0 \text{Tr}\left(1 + \nu_z\right)t^\dagger(eV_1)\nu_z t(eV_1), \tag{5.39}$$

with $G_0 = N_\Phi e^2/h$.

5.5.2 Linear response

The linear response conductance $G = \lim_{V_1 \to 0} dI_2/dV_1$ simplifies because at the Fermi level we can use the particle-hole symmetry relations

$$\left.\begin{array}{l} \nu_y\sigma_y t\nu_y\sigma_y = t^* \\ |\Psi_n^+\rangle = \nu_y\sigma_y|\Psi_n^-\rangle^* \end{array}\right\} \text{ at } E = 0. \tag{5.40}$$

These two relations imply that

$$\left.\begin{array}{l} \text{Tr}\, t^\dagger\nu_z t = 0 \\ \langle\Psi_n^+|\nu_z|\Psi_n^-\rangle = 0 \end{array}\right\} \text{ at } E = 0. \tag{5.41}$$
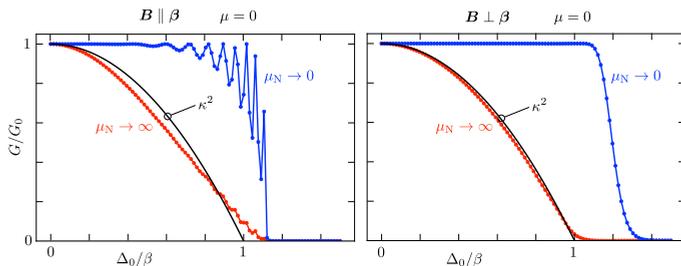
Figure 5.3: Dependence of the conductance G on the pair potential Δ_0, computed from the tight-binding model for $\boldsymbol{B}$ parallel to $\boldsymbol{\beta}$ (left panel) and for $\boldsymbol{B}$ perpendicular to $\boldsymbol{\beta}$ (right panel). The parameters are $d_0 = 18\,a_0$, $L = 30\,a_0$, and $\mu = 0$ (so there is no difference between parallel or antiparallel orientation of $\boldsymbol{B}$). The red and blue curves show the results with and without a large potential step at the NS interfaces. The black curve is the $\mu = 0$ result $G = \kappa^2 G_0$ from Ref. 97.

The equation (5.39) for the differential conductance thus reduces in linear response to

$$G = \tfrac{1}{2} G_0 \operatorname{Tr} \nu_z t^\dagger \nu_z t$$

$$= \tfrac{1}{2} G_0 \sum_{s=\pm} \langle \Psi_2^s | \nu_z | \Psi_2^s \rangle \langle \Psi_1^s | \nu_z | \Psi_1^s \rangle = N_\Phi \frac{(e^*)^2}{h}. \qquad (5.42)$$

The charge $e \mapsto e^*$ *quadratically* renormalizes the conductance [97].

Application of Eq. (5.29) at $E = 0$ then gives the result

$$G/G_0 = \begin{cases} \kappa^2 \pm (2\mu/\beta)(\kappa^2 - \kappa) & \text{if } \boldsymbol{\beta} \parallel \boldsymbol{B}, \\ \kappa^2 & \text{if } \boldsymbol{\beta} \perp \boldsymbol{B}, \end{cases} \qquad (5.43)$$

to first order in μ. The $\pm$ sign refers to $\boldsymbol{\beta}$ parallel $(+)$ or antiparallel $(-)$ to $\boldsymbol{B}$. The difference $\delta G = G(B) - G(-B)$ is thus given by the formula (5.2) announced in the introduction.

5.6 Numerical results

To test these analytical results, we have calculated the conductance numerically from a tight-binding model obtained by discretizing the Hamiltonian (7.5) of the Weyl superconductor on a cubic lattice (lattice constant
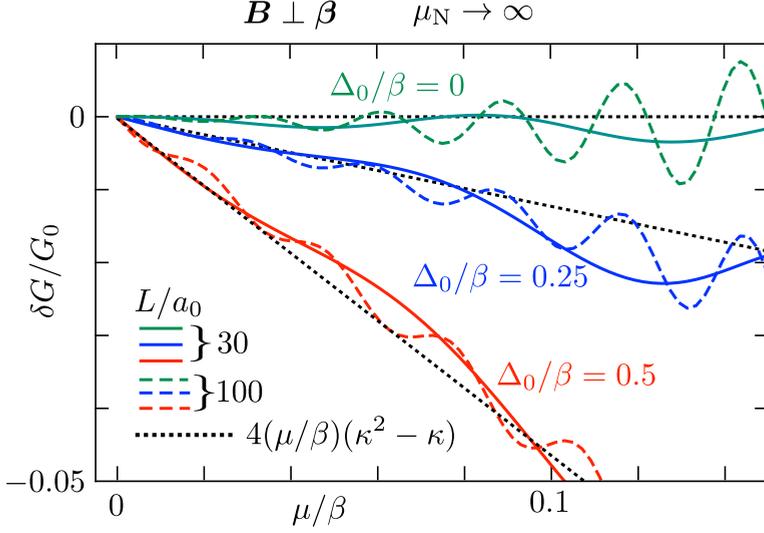
Figure 5.4: Dependence of the conductance on the orientation of $\boldsymbol{B}$, when it is perpendicular to $\boldsymbol{\beta}$ and there is a large potential step at the NS interfaces (limit $\mu_N \to \infty$). The colored curves show $\delta G = G(B) - G(-B)$ as a function of μ, computed from the tight-binding model ($d_0 = 18\,a_0$, three values of Δ_0/β, two values of L). The black dotted line is the linear μ-dependence following from Eq. (5.43).

a_0):

$$
\begin{aligned}
H_S = {} & (v_F/a_0)\tau_z \sum_{\alpha=x,y,z} \sigma_\alpha \sin(a_0 \nu_z k_\alpha - e a_0 \nu_0 A_\alpha) \\
& + \nu_0 \tau_0 \boldsymbol{\beta} \cdot \boldsymbol{\sigma} - \mu \nu_z \tau_0 \sigma_0 \\
& + \Delta_0 (\nu_x \cos\phi - \nu_y \sin\phi)\tau_0 \sigma_0 \\
& + (v_F/a_0)\nu_z \tau_x \sigma_0 \sum_{\alpha=x,y,z} (1 - \cos a_0 k_\alpha).
\end{aligned}
\tag{5.44}
$$

The term on the last line is added to avoid fermion doubling.

The vortex lattice (a square array with lattice constant d_0 and two $h/2e$ vortices per unit cell) is introduced as described in Ref. 96. The scattering matrix is calculated using the Kwant code [47], and then the linear-response conductance follows from

$$
G = \frac{I_2}{V_1} = \frac{e^2}{h} \operatorname{Tr}(t_{ee}^\dagger t_{ee} - t_{he}^\dagger t_{he}),
\tag{5.45}
$$

where the trace is taken over all the N_Φ modes in the magnetic Brillouin zone and the transmission matrices are evaluated at the Fermi level ($E = 0$).

In Fig. 5.3 we compare the conductance with and without a potential step at the NS interfaces. In the absence of a potential step, when the Hamiltonian H_N in N equals H_S with $\Delta_0 = 0$, the conductance has the bare value of $G_0 = N_\Phi e^2/h$, as long as Δ_0 remains well below β. When Δ_0 exceeds β a gap opens up at the Weyl point and the three-terminal conductance G vanishes: All the carriers injected into the superconductor by contact N_1 are then drained to ground before they reach contact N_2.

The theory developed here does not apply to this case $\mu_N = \mu$, but instead addresses the more realistic case $\mu_N \gg \mu$ of a large potential step at the NS interfaces. In the numerics we implement the large-μ_N limit by removing the transverse hoppings from the tight-binding Hamiltonian in the normal-metal leads, which is then given by

$$H_N = (v_F/a_0)\nu_z\tau_z\sigma_z \sin a_0 k_z + \nu_0\tau_0 \boldsymbol{\beta} \cdot \boldsymbol{\sigma}$$
$$+ (v_F/a_0)\nu_z\tau_x\sigma_0(1 - \cos a_0 k_z). \tag{5.46}$$

As shown in the same Fig. 5.3, in that case the conductance at $\mu = 0$ follows the predicted $\kappa^2 = 1-\Delta_0^2/\beta^2$ parabolic profile [97]. The agreement is better for $\boldsymbol{B}$ perpendicular to $\boldsymbol{\beta}$ than it is for $\boldsymbol{B}$ parallel to $\boldsymbol{\beta}$.

Fig. 5.4 is the test of our key result, the difference (5.2) of the conductance for $\boldsymbol{B}$ parallel or antiparallel to $\boldsymbol{\beta}$. The linear μ-dependence has the predicted slope, without any adjustable parameter. Backscattering from the NS interfaces produces Fabry-Perot-type oscillations around this linear dependence, more rapidly oscillating when the separation L of the NS interfaces is larger (compare dashed and solid curves).

5.7 Conclusion

In summary, we have calculated the charge e^* that Weyl fermions in a superconducting vortex lattice transport into a normal-metal contact. When the chemical potential μ in the superconductor is at the Weyl point, the transferred charge equals the charge expectation value Q_0 of the Weyl fermions [97] (in the limit of a large chemical potential μ_N in the metal contacts). There is then no dependence on the relative orientation of the magnetic field $\boldsymbol{B}$ and the separation vector $\boldsymbol{\beta}$ of the Weyl points of opposite chirality. But when $\mu \neq 0$ a dependence on $\boldsymbol{B} \cdot \boldsymbol{\beta}$ appears.

This signature of chirality shows up in the conductance, which differs if $\boldsymbol{B}$ is parallel or antiparallel to $\boldsymbol{\beta}$. It is not a large effect, a few percent

(see Fig. 5.4), but since it is specifically tied to the sign of the magnetic field it should stand out from other confounding effects.

We have taken a simple layered model for a Weyl superconductor [6], to have a definite form for the pair potential. We expect the effect to be generic for Weyl semimetals in which superconductivity is intrinsic rather than induced [7, 100]. We also expect the effect to be robust to long-range disorder scattering, in view of the chirality of the motion along the magnetic field lines (backscattering needs to couple states at $\pm K$).

Appendices

5.A Derivation of Eq. (5.18)

We wish to show that the derivative

$$\frac{d}{dz}\langle\Psi|f(\hat{k}_z)\hat{v}_z|\Psi\rangle_z$$

$$= \langle\Psi|f(\hat{k}_z)\hat{v}_z\partial_z\Psi\rangle_z + \langle\partial_z\Psi|f(\hat{k}_z)\hat{v}_z\Psi\rangle_z$$

$$= i\langle\Psi|f(\hat{k}_z)\hat{k}_z\hat{v}_z\Psi\rangle_z - i\langle\hat{k}_z\hat{v}_z\Psi|f(\hat{k}_z)\Psi\rangle_z \qquad (5.47)$$

vanishes for any function $f(\hat{k}_z)$ of $\hat{k}_z = -i\partial/\partial z$.

We rewrite

$$\hat{k}_z\hat{v}_z\Psi = (\mathcal{H} - \delta\mathcal{H})\Psi = (E - \delta\mathcal{H})\Psi \qquad (5.48)$$

and use firstly that

$$\langle\Psi_1|\delta\mathcal{H}\Psi_2\rangle_z = \langle\delta\mathcal{H}\Psi_1|\Psi_2\rangle_z, \qquad (5.49)$$

because $\delta\mathcal{H}$ does not contain any z-derivatives, and secondly that

$$[f(\hat{k}_z), \delta\mathcal{H}] = 0, \qquad (5.50)$$

because $\delta\mathcal{H}$ does not depend on z. This gives the sequence of identities

$$\langle\Psi|f(\hat{k}_z)\hat{k}_z\hat{v}_z\Psi\rangle_z = \langle\Psi|f(\hat{k}_z)(\mathcal{H} - \delta\mathcal{H})\Psi\rangle_z$$

$$= \langle\Psi|f(\hat{k}_z)(E - \delta\mathcal{H})\Psi\rangle_z$$

$$= \langle(E - \delta\mathcal{H})\Psi|f(\hat{k}_z)\Psi\rangle_z$$

$$= \langle(\mathcal{H} - \delta\mathcal{H})\Psi|f(\hat{k}_z)\Psi\rangle_z$$

$$= \langle\hat{k}_z\hat{v}_z\Psi|f(\hat{k}_z)\Psi\rangle_z. \qquad (5.51)$$

Substitution into Eq. (5.47) then proves Eq. (5.18) from the main text.